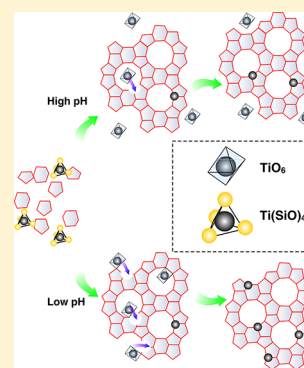


# Finding the “Missing Components” during the Synthesis of TS-1 Zeolite by UV Resonance Raman Spectroscopy

Qiang Guo,<sup>†,‡</sup> Zhaochi Feng,<sup>†</sup> Guanna Li,<sup>†</sup> Fengtao Fan,<sup>\*,†</sup> and Can Li<sup>\*,†</sup><sup>†</sup>State Key Laboratory of Catalysis, Dalian Institute of Chemical Physics, Chinese Academy of Sciences, 457 Zhongshan Road, Dalian 116023, China<sup>‡</sup>Graduate University of Chinese Academy of Sciences, Beijing 100049, China

## Supporting Information

**ABSTRACT:** The catalytic performance of TS-1 zeolite greatly depends on the types of titanium species and their concentrations in the zeolite. Coupled with UV/vis spectroscopy, we present a UV resonance Raman spectroscopic investigation on the evolution of the titanium species during the crystallization of TS-1 zeolite. It is found that a small portion of Ti species leaches from the solid phase into the liquid phase. The “missing” Ti species in addition to the framework Ti species during the assembly process of TS-1 is identified as isolated “TiO<sub>6</sub>” species, due to the resonance Raman effect excited at 266 nm. The formation mechanisms of framework Ti species in TS-1 and the relation with the isolated “TiO<sub>6</sub>” species during the synthesis process are clarified. A synthetic strategy was designed to increase the concentration of the framework titanium by a factor of 1.5 for the actual synthesis of TS-1 zeolite.



## INTRODUCTION

The TS-1 zeolite is considered a milestone in heterogeneous catalysis fields due to its excellent performance in a large number of oxidation reactions, using H<sub>2</sub>O<sub>2</sub> as oxidant under mild conditions.<sup>1–9</sup> The catalytic performance of TS-1 zeolite greatly depends on the type and content of titanium incorporated into it. It is, however, worth noting that only small amounts of titanium (usually less than 2 wt %) can be incorporated into the zeolite framework, despite using extremely pure reagents and under severely controlled synthesis conditions.<sup>5,6,10,11</sup> To increase the amount of the titanium in TS-1 zeolite is still a challenge. One important reason accounts for the difficulty of titanium insertion into the framework due to the much longer Ti–O bond as compared to that of the Si–O bond,<sup>5,13–15</sup> and a large amount of the Ti species in the initial gel is leaching into the liquid solutions during the synthesis.

Extensive studies have been made for the study on this subject.<sup>5,6,8,10,12</sup> Among these studies, employing the crystallization-mediating agent (e.g., isopropyl alcohol, hydrogen peroxide), which can promote the Ti insertion to the zeolite, is an effective way to increase the lattice Ti content.<sup>8,10,12</sup> In this respect, Fan et al. reported that the presence of (NH<sub>4</sub>)<sub>2</sub>CO<sub>3</sub> in the crystallization gel can considerably increase the framework Ti content by harmonizing the crystallization speed and the rate of Ti insertion into the framework.<sup>5,6</sup> Despite these efforts, a clear understanding of the incorporation mechanism of framework titanium species at the molecular level is still lacking.

However, information on the coordination environment of Ti species is hard to obtain due to the extremely low metal concentration. A variety of techniques have been employed to

characterize the coordination state of the titanium species in the TS-1 zeolite: With increasing Ti content in the framework of silicate, the cell volume values resulting from Rietveld refinements of the X-ray powder diffraction data increase proportionally.<sup>5,16,17</sup> The intensity of the distinctive IR absorption component centered at 960 cm<sup>-1</sup> was assumed to be correlated with the tetrahedral framework titanium content.<sup>5,15,18</sup> The intensity of the pre-edge peak around the Ti K edge at 4967 eV of the XANES spectra has been also employed to detect the tetrahedral framework titanium in TS-1 according to the 1s–3pd electronic transition involving Ti(IV) atoms, and EXAFS spectroscopy has been widely used to determine the local bonding parameters around the titanium.<sup>15,19,20</sup>

A powerful tool to address this issue is UV resonance Raman spectroscopy. With resonance Raman effect, the Ti species with extremely low concentration in different coordination environments are successfully identified.<sup>21–26</sup> In addition, UV Raman spectroscopy has been demonstrated to be a suitable tool for the characterization of zeolites due to decreased fluorescence and increased sensitivity, especially for monitoring intermediates involved in zeolite framework formation.<sup>27–29</sup>

In this work, the evolution of the titanium species during the crystallization of TS-1 zeolite was monitored by UV Raman spectroscopy in combination with UV/vis spectroscopy, X-ray diffraction patterns, and inductively coupled plasma atomic emission spectroscopy. Two different Ti species involved in

Received: November 4, 2012

Revised: January 14, 2013

Published: January 14, 2013

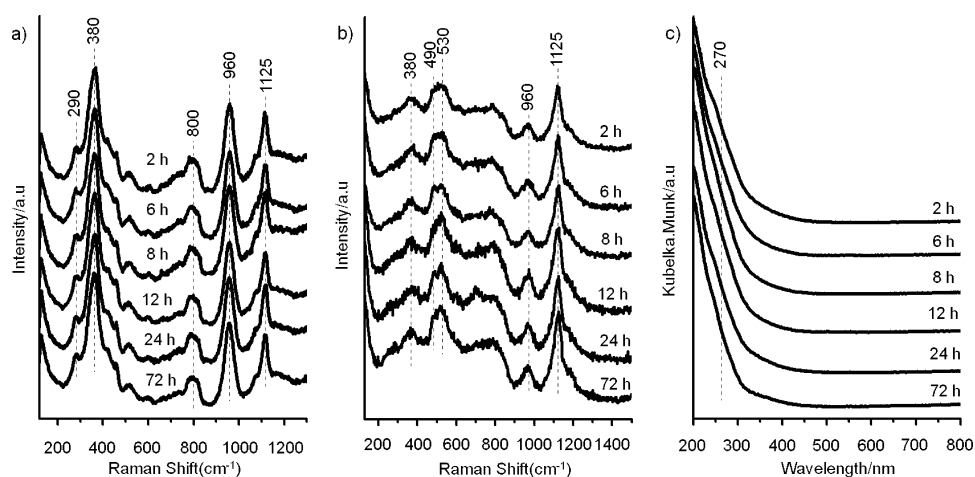


**Figure 1.** UV Raman spectra excited at (a) 325 nm, (b) 244 nm, and (c) UV-vis spectra of TS-1 zeolite (Si/Ti = 50) for different crystallization stages at various times of synthesis.

TS-1 synthesis and the relation between the two species derived during the synthesis process are clarified. Besides, a synthetic strategy to control the titanium species based on knowledge obtained from the studies is proposed.

## EXPERIMENTAL SECTION

**Materials Synthesis.** TS-1 samples were synthesized with a modified procedure according to the literature.<sup>5,30</sup> TS-1 was prepared from a starting titaniumsilicate gel with a molar ratio of 1.0SiO<sub>2</sub>/0.02TiO<sub>2</sub>/0.5TPAOH/35H<sub>2</sub>O. A typical run consisted of several steps: 0.16 g of titanium tetra-*n*-butoxide (TBOT) was first added to an aqueous solution of H<sub>2</sub>O<sub>2</sub> (5 mL), followed by the addition of 9.6 g of 20 wt % aqueous solution of tetrapropylammonium hydroxide (TPAOH). The tetraethyl orthosilicate (4 g) was added to the solution after 30 min. Next, the solution was heated in a water bath kept at 55 °C for about 4 h. After the alcohol was evaporated, a certain amount of water was added to compensate for the vaporized portion. Glycine was added to adjust the pH value of the gel. Crystallization was completed in stainless steel autoclaves (20 mL) for 72 h at 170 °C. The solid product was centrifugated, washed with distilled water and alcohol (1 g/15 mL), and then dried at 80 °C overnight. In some cases, the dried sample was treated with 1 M HCl (1 g/50 mL) for 24 h. All of the samples were calcined at 550 °C for 10 h.

To investigate the evolution of titanium species during TS-1 formation, the autoclaves were put into an oven at 170 °C for crystallization, and then quenched at given periods of time by an ice bath. The solid samples were centrifuged to separate them from the mother liquid, washed with deionized water, dried at 80 °C, and calcined at 550 °C.

**Characterizations.** UV Raman spectra were recorded on a home-assembled UV Raman spectrograph using a Jobin-Yvon T64000 triplestage spectrograph with spectral resolution of 2 cm<sup>-1</sup>. The laser line at 325 nm of a He–Cd laser was used as exciting source with an output of 50 mW. The power of the laser at samples was about 1.0 mW. The 244 nm line from a Coherent Innova 300 Fred laser and the line at 266 nm from the double-frequency of a DPSS 532 model 200 532 nm laser were also used as excitation source. The power of the 244 and 266 nm lines at samples was below 1.0 mW.

XRD patterns were recorded on a Rigaku RINT D/Max-2500 powder diffraction system using Cu K $\alpha$  radiation (40 kV

and 50 mA). The diffuse reflectance (DR) UV-vis spectra were measured on a Jasco V-550 UV-vis spectrophotometer with a BaSO<sub>4</sub> plate as the reference. The chemical compositions of the samples were determined by a Shimadzu ICPS-8100 inductively coupled plasma atomic emission spectrometer (ICP).

## RESULTS AND DISCUSSION

Figure 1a shows the UV Raman spectra of the products excited at 325 nm. All samples show the characteristic bands of the MFI structure at 290, 380, and 800 cm<sup>-1</sup> after crystallization for 2 h. The result meets well with the XRD pattern characterization in Figure S1. Besides, the Raman spectra of the samples show Raman bands at 960 and 1125 cm<sup>-1</sup>, which arise from the asymmetric stretching and the symmetric stretching vibration of the framework TiO<sub>4</sub> unit, respectively.<sup>21,31</sup> No Raman bands at 144, 390, and 637 cm<sup>-1</sup> are observed in all spectra, indicating that there are no anatase-like species in the samples. The existence of the framework TiO<sub>4</sub> unit in all samples is further confirmed by the resonance Raman spectra excited at 244 nm, as shown in Figure 1b. The Raman spectra of the samples show strong Raman bands at 490, 530, and 1125 cm<sup>-1</sup>, which have been assigned to the symmetric stretching and asymmetric stretching vibrations of framework Ti–O–Si species.<sup>21,31</sup> By prolonging the crystallization time, the resonance Raman bands at 1125 cm<sup>-1</sup> become narrower. This result demonstrates that the coordination environment of the framework titanium becomes more rigid and uniform.

Although some changes in the coordination state of Ti species are detected by the UV Raman spectroscopy excited at 244 and 325 nm, no clear-cut conclusion could be made due to the small variations. The situation did not improve after collecting the UV/vis spectra of the samples, as shown in Figure 1c. The UV/vis spectra of all of the samples synthesized at different time intervals exhibit a similar contour: a standing strong band at 210 nm and a weak shoulder band at 270 nm with small variations. The band at 210 nm is a characteristic band of the framework titanium species in tetrahedral coordination environment,<sup>5</sup> while the band at 270 nm is assigned to the isolated octahedral titanium species according to the previous study.<sup>26</sup> The different titanium species could be well differentiated through the resonance Raman effect by shifting the excitation laser lines toward their UV-vis bands.

To obtain a clear understanding of the evolution of the titanium species during synthesis, the entire process was monitored by UV Raman spectroscopy excited at 266 nm (Figure 2). The synthesis gels within 2 h of crystallization are

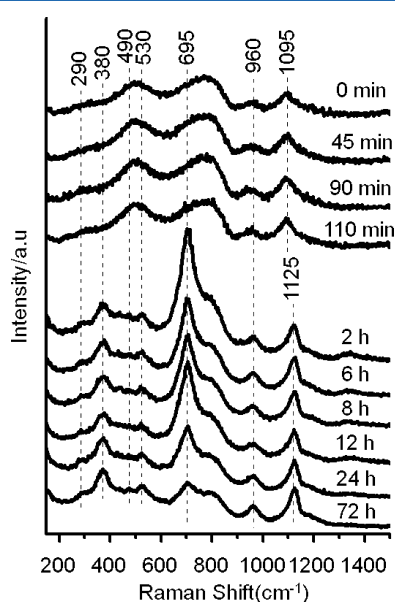


**Figure 2.** UV Raman spectra excited at 266 nm of TS-1 zeolite (Si/Ti = 50) for the whole crystallization stage at various times of synthesis.

clear solutions. The UV Raman spectra of these synthesis gels are almost the same: the spectra are characterized by a distinct Raman band at  $1095\text{ cm}^{-1}$  and several other broad bands at 500 and  $960\text{ cm}^{-1}$ , indicating the existence of tetrahedrally coordinated  $\text{Ti}(\text{OSi})_4$  species in the early stage of synthesis.<sup>24</sup> However, these Ti species are not as rigidly coordinated as those in well-crystallized zeolite frameworks because the characteristic bands at  $1095\text{ cm}^{-1}$  are shifted to lower frequency as compared to that at  $1125\text{ cm}^{-1}$  in fully crystallized TS-1 zeolite. After crystallization for 2 h, the clear solution of the synthesis gel becomes heterogeneous. The spectra of the solid phase give Raman bands at  $380$  and  $1125\text{ cm}^{-1}$ . The result reflects that the MFI framework is formed and the Ti species in tetrahedral coordination become rigidly coordinated.

The Raman band at  $695\text{ cm}^{-1}$ , which arises from the isolated octahedral titanium species, appears after 2 h of crystallization, and its intensity decreases with prolonged synthesis time. According to our experiment, acid washing is an effective way to remove the octahedral titanium species while maintaining the tetrahedral framework titanium. The result is further confirmed by the Raman spectra of the acid-treated samples (Figure S2). The concentrations of the total amount of titanium and the tetrahedral framework titanium in the products before and after acid washing were determined by ICP-AES, respectively. As shown in Figure 3a, the ratios of Ti to (Ti+Si) are decreasing for both the total amount of titanium (Figure 3a, trace 2) and the tetrahedral framework titanium (Figure 3a, trace 1) in the solid phase with the increasing synthesis time. However, the amount of framework Ti is smaller than that of the total amount of Ti atoms, and the differences become smaller with increasing synthesis time. Finally, these two ratios reach the same value after 72 h of synthesis. Notice that the decreasing intensity of the Raman band at  $695\text{ cm}^{-1}$  is accompanied by the crystallization of the

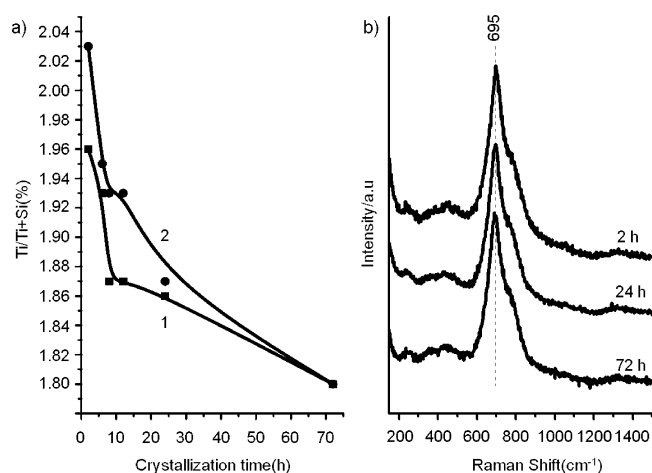


**Figure 3.** (a) Ti/Ti+Si ratio of the solid phase for different crystallization stages at various times of the synthesis: (1) the solid phase is washed with HCl, (2) without HCl treatment; and (b) UV Raman spectra of the liquid phase excited at 266 nm for different crystallization stages at various times of the TS-1 zeolite (Si/Ti = 50) synthesis.

Ti species in tetrahedral coordination, as evidenced by the sharpening of the Raman band at  $1125\text{ cm}^{-1}$  in Figure 1b. Thus, a reasonable explanation of this process should be that a small number of Ti species in tetrahedral coordination is extruded in the form of isolated “ $\text{TiO}_6$ ” species. This kind of “ $\text{TiO}_6$ ” species is attached to the solid phase of the synthesis mixture. With the solid phase becoming fully crystallized, “ $\text{TiO}_6$ ” species drop off from the crystals gradually. This explanation is also supported by the fact that the liquid phase of the synthesis gel after 2 h of crystallization is dominated by the Raman band at  $695\text{ cm}^{-1}$  (Figure 3b) and the different decreasing trends of total amount of titanium and framework titanium in the solid phase with increasing synthesis time (Figure 3a).

Thus, the incorporation process of titanium species into TS-1 zeolite is described as follows: At the early stage of the crystallization, the Ti is tetrahedrally coordinated with  $\text{SiO}_4$  units, characterized by the Raman bands at  $500$  and  $1095\text{ cm}^{-1}$ . By prolonging the synthesis time, the Ti species in tetrahedral coordination aggregate with the silicate species to form the zeolite framework. By increasing the synthesis time, the Ti–Si distance shortens, and the coordination environment of the Ti becomes more rigid. What we are learning here is a small number of Ti species in tetrahedral coordination is extruded from the framework in the form of isolated “ $\text{TiO}_6$ ” species during the framework formation while the others incorporate into the framework. The “ $\text{TiO}_6$ ” species is attached to the solid phase and dissolved into the liquid phase gradually with increasing the synthesis time. Meanwhile, the coordination environment of the framework Ti species in tetrahedral coordination becomes more rigid.

As we have observed in the synthesis process, some Ti species are extruded from the framework. If this kind of titanium species could be incorporated into the framework, the content of framework titanium should be further increased. The extrusion of the Ti species due to the mismatch between the Ti–O bond and the Si–O bond hampers the insertion of titanium into the zeolite framework, particularly when the zeolite framework crystallizes too fast. A proper way to solve this problem is to reduce the pH value of the synthesis gel,

which could decrease the speed of the crystallization.<sup>5</sup> Herein, glycine is employed to control the crystallization speed, and the condensation speed of titanasilicate and silicate species. All of the TS-1 materials synthesized with different glycine contents show high crystallinity of the MFI structure, as confirmed by X-ray diffraction patterns (Figure S3). Also, the X-ray diffraction patterns of TS-1 zeolite (Si/Ti = 50) for the whole crystallization stage at various times of synthesis at pH = 10.5 were given in Figure S4. As compared to the crystallization process without glycine (pH = 12), the crystallization rate with glycine (pH = 10.5) was obviously retarded. As discussed above, this should result from the fact that the pH value was lowered with the addition of the glycine. After the addition of a certain amount of glycine, the pH value lowers from 12 to 10.5 and remains around 10.5 during the whole process of crystallization (Figure 4). In contrast, the pH value in the

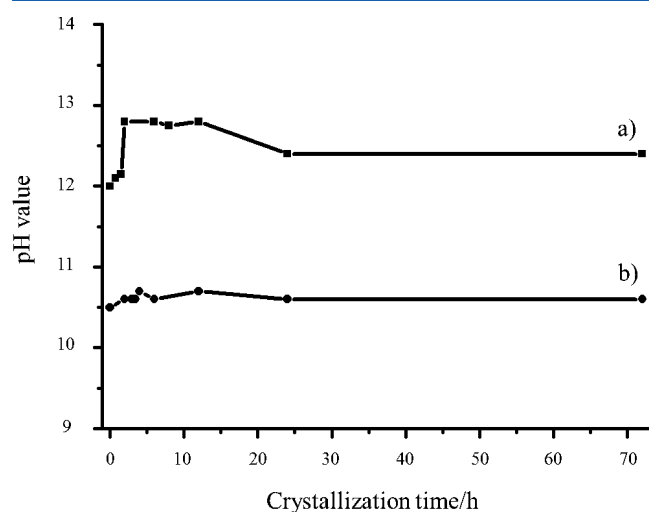


**Figure 4.** Evolution of the pH value of the liquid fraction during the crystallization process of TS-1 at (a) pH = 12 and (b) pH = 10.5.

liquor phase without addition of glycine presents a sudden increase from 12.1 to 12.8 in the very early stages of the synthesis, and then decreased to 12.4 with prolonged synthesis time. The incorporation of the silicate species into the zeolite framework, which releases the OH<sup>-</sup>, results in the increase of the pH value. The higher pH value will further accelerate the zeolite growth. Thus, the addition of the glycine decreases the pH value and serves as a buffer reagent through the crystallization process, resulting in the decreased crystallization speed.

Figure 5a shows the UV Raman spectra of TS-1 synthesized at different pH values excited at 244 nm. With lowering the pH value of the synthesis gel through the addition of glycine, the intensity of the Raman band at 1125 cm<sup>-1</sup> increases obviously, reflecting the increasing amount of framework titanium species. According to the ICP-AES analysis and the intensities of the Raman band at 1125 cm<sup>-1</sup> (by using the intensity of the Raman band at 380 cm<sup>-1</sup> as an interior label), the concentration of the framework Ti is increased by a factor of 1.5 from TS-1 (pH = 12) to TS-1 (pH = 10.2).

Another finding is that by lowering the pH value of the synthesis gel, the Raman bands at 695 cm<sup>-1</sup> from the TiO<sub>6</sub> species are observed when excited at 266 nm, as shown in Figure 5b. It should be mentioned that the absorption band at 270 nm in the UV-vis spectrum is invisible for the sample

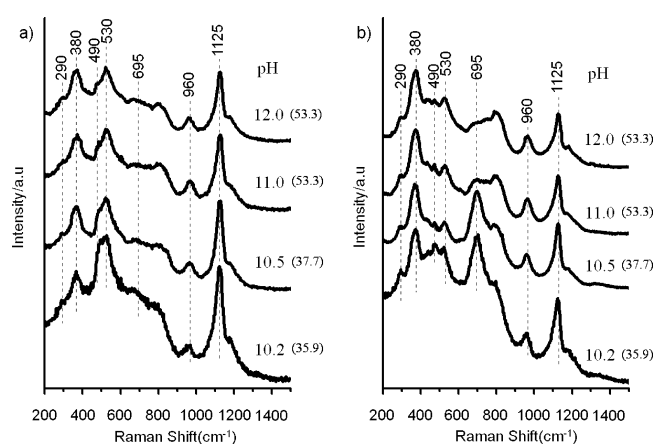


**Figure 5.** UV resonance Raman spectra of TS-1 zeolite synthesized at different pH values excited at (a) 244 nm and (b) 266 nm. (The Si/Ti ratios analyzed by ICP-AES are listed in parentheses.)

synthesized at pH = 12, 11, and 10.5, indicating the extreme low concentration of the extra framework species. However, these species are stably attached to TS-1 crystals and cannot be removed even by HCl treatment. The results reflect that, at lower pH values, the speed of the zeolite crystallization decreases and the Ti–O–Si bonds became more stable.<sup>5</sup> In such a manner, titanium in the synthesis gel could be incorporated into the zeolite framework effectively, and the formed TiO<sub>6</sub> species in extremely low amount is hard to dissolve into the liquid phase. As a conclusion, lowering the pH value of the synthesis gel through the addition of glycine is an efficient way to increase the amount of framework titanium.

## CONCLUSION

Incorporating processes of the titanium species in different coordination into the MFI-type zeolite were well studied by UV resonance Raman spectroscopy with finely tuned excitation lasers. The results show that, in the initial gel, the Ti atoms are tetrahedrally coordinated with SiO<sub>4</sub> units, which then aggregate with the silicate species to form a solid phase. With increasing synthesis time, the coordination environment of the Ti becomes more rigid. Meanwhile, a small number of Ti species in tetrahedral coordination convert into the liquid phase in the form of isolated “TiO<sub>6</sub>” species gradually. It is found that, by lowering the pH value of the synthesis gel, the conversion of Ti species in tetrahedral coordination into “TiO<sub>6</sub>” can be depressed due to the increased stability of the Ti–O–Si bonds. This improvement can lead to the increasing of the framework Ti by a factor of 1.5.

## ASSOCIATED CONTENT

### Supporting Information

X-ray diffraction patterns of TS-1 zeolite (Si/Ti = 50) for the whole crystallization stage at various times of synthesis, UV Raman spectra excited at 266 nm of TS-1 zeolite (Si/Ti = 50) for different crystallization stages at various times of synthesis, X-ray diffraction patterns of TS-1 zeolite (Si/Ti = 50) synthesized at different pH values, X-ray diffraction patterns of TS-1 zeolite (Si/Ti = 50) for the whole crystallization stage at various times of synthesis with addition of glycine (pH = 10.5), and <sup>29</sup>Si MAS NMR spectra of TS-1 zeolite (Si/Ti = 50) for different crystallization stages at various times of synthesis (pH = 12).



This material is available free of charge via the Internet at <http://pubs.acs.org>.

## AUTHOR INFORMATION

### Corresponding Author

\*Phone: +86-411-84379070. Fax: +86-411-84694447. E-mail: [ftfan@dicp.ac.cn](mailto:ftfan@dicp.ac.cn) (F.F.). E-mail: [canli@dicp.ac.cn](mailto:canli@dicp.ac.cn) (C.L.).

### Notes

The authors declare no competing financial interest.

## ACKNOWLEDGMENTS

This work was financially supported by the National Natural Science Foundation of China (21003122), the National Basic Research Program of China (2009CB623507), and Programme Strategic Scientific Alliances between China and The Netherlands (2008DFB50130).

## REFERENCES

- (1) Taramasso, M.; Perego, G.; Notari, B. *Snampoprogetti Spa (Snam) Anic Spa (Anis)* **1983**, 9.
- (2) Clerici, M. G.; Ingallina, P. *J. Catal.* **1993**, *140*, 71–83.
- (3) Khouw, C. B.; Davis, M. E. *J. Catal.* **1995**, *151*, 77–86.
- (4) Notari, B. *Adv. Catal.* **1996**, *41*, 253–334.
- (5) Fan, W. B.; Duan, R. G.; Yokoi, T.; Wu, P.; Kubota, Y.; Tatsumi, T. *J. Am. Chem. Soc.* **2008**, *130*, 10150–10164.
- (6) Fan, W. B.; Fan, B. B.; Shen, X. H.; Li, J. F.; Wu, P.; Kubota, Y.; Tatsumi, T. *Microporous Mesoporous Mater.* **2009**, *122*, 301–308.
- (7) Barbera, D.; Cavani, F.; D'Alessandro, T.; Fornasari, G.; Guidetti, S.; Aloise, A.; Giordano, G.; Piumetti, M.; Bonelli, B.; Zanzottera, C. *J. Catal.* **2010**, *275*, 158–169.
- (8) Shan, Z. C.; Lu, Z. D.; Wang, L.; Zhou, C.; Ren, L. M.; Zhang, L.; Meng, X. J.; Ma, S. J.; Xiao, F. S. *ChemCatChem* **2010**, *2*, 407–412.
- (9) Shan, Z. C.; Wang, H.; Meng, X. J.; Liu, S. Y.; Wang, L. A.; Wang, C. Y.; Li, F.; Lewis, J. P.; Xiao, F. S. *Chem. Commun.* **2010**, *47*, 1048–1050.
- (10) Thangaraj, A.; Sivasanker, S. *J. Chem. Soc., Chem. Commun.* **1992**, 123–124.
- (11) Lamberti, C.; Bordiga, S.; Zecchina, A.; Artioli, G.; Marra, G.; Spano, G. *J. Am. Chem. Soc.* **2001**, *123*, 2204–2212.
- (12) Tamura, M.; Chaikittisilp, W.; Yokoi, T.; Okubo, T. *Microporous Mesoporous Mater.* **2008**, *112*, 202–210.
- (13) Blasco, T.; Cambor, M. A.; Corma, A.; Pérez Pariente, J. *J. Am. Chem. Soc.* **1993**, *115*, 11806–11813.
- (14) Lamberti, C.; Bordiga, S.; Arduino, D.; Zecchina, A.; Geobaldo, F.; Spano, G.; Genoni, F.; Petrini, G.; Carati, A.; Villain, F.; et al. *J. Phys. Chem. B* **1998**, *102*, 6382–6390.
- (15) Bordiga, S.; Bonino, F.; Damin, A.; Lamberti, C. *Phys. Chem. Chem. Phys.* **2007**, *9*, 4854–4878.
- (16) Millini, R.; Massara, E. P.; Perego, G.; Bellussi, G. *J. Catal.* **1992**, *137*, 497–503.
- (17) Lamberti, C.; Bordiga, S.; Zecchina, A.; Carati, A.; Fitch, A. N.; Artioli, G.; Petrini, G.; Salvalaggio, M.; Marra, G. L. *J. Catal.* **1999**, *183*, 222–231.
- (18) Marra, G. L.; Artioli, G.; Fitch, A. N.; Milanesio, M.; Lamberti, C. *Microporous Mesoporous Mater.* **2000**, *40*, 85–94.
- (19) Bordiga, S.; Boscherini, F.; Coluccia, S.; Genoni, F.; Lamberti, C.; Leofanti, G.; Marchese, L.; Petrini, G.; Vlaic, G.; Zecchina, A. *Catal. Lett.* **1994**, *26*, 195–208.
- (20) Bordiga, S.; Coluccia, S.; Lamberti, C.; Marchese, L.; Zecchina, A.; Boscherini, F.; Buffa, F.; Genoni, F.; Leofanti, G.; Petrini, G.; et al. *J. Phys. Chem.* **1994**, *98*, 4125–4132.
- (21) Li, C.; Xiong, G.; Xin, Q.; Liu, J. K.; Ying, P. L.; Feng, Z. C.; Li, J.; Yang, W. B.; Wang, Y. Z.; Wang, G. R.; et al. *Angew. Chem., Int. Ed.* **1999**, *38*, 2220–2222.
- (22) Li, C.; Xiong, G.; Liu, J. K.; Ying, P. L.; Xin, Q.; Feng, Z. C. *J. Phys. Chem. B* **2001**, *105*, 2993–2997.
- (23) Li, C. *J. Catal.* **2003**, *216*, 203–212.

- (24) Fan, F. T.; Feng, Z. C.; Li, C. *Acc. Chem. Res.* **2010**, *43*, 378–387.
- (25) Fan, F. T.; Feng, Z. C.; Li, C. *Chem. Soc. Rev.* **2010**, *39*, 4794–4801.
- (26) Guo, Q.; Sun, K. J.; Feng, Z. C.; Li, G. N.; Guo, M. L.; Fan, F. T.; Li, C. *Chem.-Eur. J.* **2012**, *18*, 13854–13860.
- (27) Fan, F. T.; Feng, Z. C.; Li, G. N.; Sun, K. J.; Ying, P. F.; Li, C. *Chem.-Eur. J.* **2008**, *14*, 5125–5129.
- (28) Fan, F. T.; Feng, Z. C.; Sun, K. J.; Guo, M. L.; Guo, Q.; Song, Y.; Li, W. X.; Li, C. *Angew. Chem., Int. Ed.* **2009**, *48*, 8743–8747.
- (29) Fan, F. T.; Sun, K. J.; Feng, Z. C.; Xia, H. A.; Han, B.; Lian, Y. X.; Ying, P. L.; Li, C. *Chem.-Eur. J.* **2009**, *15*, 3268–3276.
- (30) Clerici, M. G.; Bellussi, G.; Romano, U. *J. Catal.* **1991**, *129*, 159–167.
- (31) Ricchiardi, G.; Damin, A.; Bordiga, S.; Lamberti, C.; Spano, G.; Rivetti, F.; Zecchina, A. *J. Am. Chem. Soc.* **2001**, *123*, 11409–11419.